

## **SANDIA REPORT**

SAND2016-6644

Unlimited Release

April 2016

# **Additive Manufacturing of Polymers: Materials Opportunities and Emerging Applications**

Hayden Thompson Black, Mathias C. Celina, James R. McElhanon

Prepared by  
Sandia National Laboratories  
Albuquerque, New Mexico 87185 and Livermore, California 94550

Sandia National Laboratories is a multi-program laboratory managed and operated by Sandia Corporation, a wholly owned subsidiary of Lockheed Martin Corporation, for the U.S. Department of Energy's National Nuclear Security Administration under contract DE-AC04-94AL85000.

Approved for public release; further dissemination unlimited.



**Sandia National Laboratories**

Issued by Sandia National Laboratories, operated for the United States Department of Energy by Sandia Corporation.

**NOTICE:** This report was prepared as an account of work sponsored by an agency of the United States Government. Neither the United States Government, nor any agency thereof, nor any of their employees, nor any of their contractors, subcontractors, or their employees, make any warranty, express or implied, or assume any legal liability or responsibility for the accuracy, completeness, or usefulness of any information, apparatus, product, or process disclosed, or represent that its use would not infringe privately owned rights. Reference herein to any specific commercial product, process, or service by trade name, trademark, manufacturer, or otherwise, does not necessarily constitute or imply its endorsement, recommendation, or favoring by the United States Government, any agency thereof, or any of their contractors or subcontractors. The views and opinions expressed herein do not necessarily state or reflect those of the United States Government, any agency thereof, or any of their contractors.

Printed in the United States of America. This report has been reproduced directly from the best available copy.

Available to DOE and DOE contractors from

U.S. Department of Energy  
Office of Scientific and Technical Information  
P.O. Box 62  
Oak Ridge, TN 37831

Telephone: (865) 576-8401  
Facsimile: (865) 576-5728  
E-Mail: [reports@osti.gov](mailto:reports@osti.gov)  
Online ordering: <http://www.osti.gov/scitech>

Available to the public from

U.S. Department of Commerce  
National Technical Information Service  
5301 Shawnee Rd  
Alexandria, VA 22312

Telephone: (800) 553-6847  
Facsimile: (703) 605-6900  
E-Mail: [orders@ntis.gov](mailto:orders@ntis.gov)  
Online order: <http://www.ntis.gov/search>



# **Additive Manufacturing of Polymers: Materials Opportunities and Emerging Applications**

Hayden T. Black, Mathias C. Celina, James R. McElhanon  
Organic Materials Science Dept. 1853  
Sandia National Laboratories  
P.O. Box 5800  
Albuquerque, New Mexico 87185-MS1411

## **Abstract**

Additive manufacturing (AM) has enabled the rapid prototyping of structures with complex geometries constructed via computer aided design (CAD). In recent years, AM has extended beyond simple prototyping and has begun to play a role in the fabrication of active components, especially for applications that do not require materials with robust mechanical properties (i.e. electronic components and biomedical scaffolds). This report reviews the current state of 3D printing with respect to polymeric and composite materials, focusing on applications, printing processes, and material selection perspectives. A particular focus is placed on the polymer chemistry of additive manufacturing in order to elucidate current materials limitations, R&D trends and developmental opportunities. Some unconventional thermoset cure reactions are proposed for AM which may overcome current limitations. In addition, potential degradation characteristics of AM polymer materials and expected property variations in comparison with traditional processing are discussed, which draws attention to the complexity of the structure/processing/property relationships for the optimization of innovative materials. AM polymer manufacturing and 3D printing approaches hold tremendous promises as long as polymer chemistry, material physics and processing aspects (cure on demand) are jointly embraced within evolving research strategies.



## CONTENTS

Materials Opportunities and Emerging Applications .....	3
Contents .....	5
Figures .....	5
Tables .....	6
Nomenclature .....	7
1. Introduction .....	9
2. Printing methods .....	11
2.1. Fused-Deposition Modelling .....	11
2.2. Stereolithography .....	14
2.3. Direct-Write .....	16
2.4. Continuous Liquid Interface Production .....	18
2.5. Selective Laser Sintering .....	19
3. The chemistry of additive manufacturing: Old and new .....	21
3.1. Monomers .....	21
3.2. Radical Photoinitiators .....	22
3.3. Photoacid Generators (Cationic Initiators) .....	23
3.4. Photobase Generators .....	24
3.5. Thermally Latent Base Catalysts .....	26
3.6. Photoclick Reactions .....	27
3.7. Unusual Polymer Materials in Additive Manufacturing .....	28
4. Material Performance and aging Considerations for Additively manufactured polymers .....	31
5. Conclusions .....	33
4. References .....	35

## FIGURES

Figure 1. Illustration of FDM process ( <a href="http://www.slideshare.net/johnbrittas/rapid-prototyping-technologiesapplications-part-deposition-planning-2">http://www.slideshare.net/johnbrittas/rapid-prototyping-technologiesapplications-part-deposition-planning-2</a> ). .....	12
Figure 2. Illustration of stereolithography process ( <a href="https://en.wikipedia.org/wiki/Stereolithography#/media/File:Stereolithography_apparatus_vector.svg">https://en.wikipedia.org/wiki/Stereolithography#/media/File:Stereolithography_apparatus_vector.svg</a> ) .....	15
Figure 3. Illustration of the direct-write printing process ( <a href="http://proto3000.com/polyjet-3d-printing-services-process.php">http://proto3000.com/polyjet-3d-printing-services-process.php</a> ) .....	16
Figure 4. (a) Illustration of CLIP components and printing technique. (b) Photographs of CLIP printer and printed component. ( <a href="http://www.carbon3D.com">www.carbon3D.com</a> ) .....	18
Figure 5. Illustration of the selective laser sintering process ( <a href="http://rapidprototypingservicescanada.com">http://rapidprototypingservicescanada.com</a> ) .....	19
Figure 6. Common monomers used in stereolithography and direct-write resins .....	21

Figure 7. Type I and Type II radical photoinitiators .....	23
Figure 8. Commercially available PAGs and their photodecomposition products .....	24
Figure 9. Amine photobase generators .....	25
Figure 10. Epoxy/thiol cure using ammonium salt PBG (left, Ref 32) and amidine PBG (right, Ref 36) .....	26
Figure 11. Thermal decomposition of retro Michael addition latent base initiator for epoxide ring opening .....	27
Figure 12. Photo click reactions with potential for additive manufacturing processes .....	28
Figure 13. SEM cross section image of printed 70% oil phase emulsion after infiltration with silver nanoparticles, showing the objects inner bulk (a) and surface (b). (Ref 41) .....	29
Figure 14. Illustration of the electric poling-assisted AM method for printing piezoelectric PVDF components (left). Image of printed PVDF device and output current and capacitive charge during flex cycles (right). (Ref 42) .....	29
Figure 15. Schematic of mechanochemical transformation from colorless spirobifluorene form to the purple colored merocyanine form (top) and images of spirobifluorene-PCL dog-bones before and after stretching. (Ref 43) .....	30

## TABLES

Table 1. Mechanical properties of FDM printed thermoplastics .....	13
Table 2. Bulk mechanical properties of selected thermoplastics .....	13
Table 3. Mechanical properties of commercially available SLA materials .....	15
Table 4. Mechanical properties of commercially available direct-write materials .....	17

## NOMENCLATURE

2PA	two-photon absorption
AM	additive manufacturing
ABS	acrylonitrile-butadiene-styrene
ASA	acrylonitrile-styrene-acrylate
CNC	computer numerical control
CAD	computer-aided design
CADD	computer-aided design and drafting
CLIP	continuous liquid interface production
DBN	1,5-diaza-bicyclo[4.3.0]non-5-ene
FDM	fused deposition modelling
IR	infrared
LLNL	Lawrence Livermore National Laboratory
MPa	megapascal
PAG	photoacid generator
PBG	photobase generator
PC	polycarbonate
PCL	polycaprolactone
PLA	polylactic acid
PEEK	polyether ether ketone
PEKK	polyether ketone ketone
PMMA	poly(methyl methacrylate)
PVDF	poly(vinylidene fluoride)
SLA	stereolithography
SLS	selective laser sintering
$T_g$	glass transition temperature
TBD	triazabicyclo[4.4.0]dec-5-ene
UV	ultraviolet



## 1. INTRODUCTION

Compared to traditional manufacturing methods for polymeric materials such as injection molding, thermoforming, extrusion, casting, foaming, as well as computer numerical control (CNC) milling, additive manufacturing represents a fundamentally different approach whereby individual layers are deposited sequentially in order to build up a 3-dimensional structure. This allows the production of complex geometries that are not easily attainable via subtractive manufacturing techniques. Additive manufacturing is particularly advantageous for small batch size production and developmental activities, since tooling and long lead times are eliminated in the manufacturing process. This allows for a closer link between the user and the manufacturing stage, opening the doors for customized printed parts which take advantage of computer-aided design and drafting (CADD). This has made AM competitive in areas where there is an inherent need for custom-made products or where low volume tailored parts are attractive to the customer. One of the earliest commercial applications of 3D printed organic materials, developed in the early 1990s, was for the fabrication of pharmaceutical capsules comprised of a drug and a polymer binder.<sup>1</sup> While this remains an active area of research and development,<sup>2</sup> a number of additional medical applications have emerged which take advantage of the geometric flexibility of 3D printing. For example, AM has become an important technology in the field of dental materials used for orthotics, implants, and prosthetics,<sup>3</sup> where customized geometries are needed for patient specifications. Other medical applications of 3D printing include regeneration scaffolds,<sup>4</sup> implantable devices such as hearing aids,<sup>5</sup> and also for pre-surgical planning purposes.<sup>6</sup> Somewhat less developed applications for 3D printed polymers include electronics,<sup>7</sup> photonics,<sup>8</sup> and microfluidics.<sup>9</sup>

While additive manufacturing has generated a surge of excitement across many fields, there are several challenges that have limited commercial utilization of AM technology. Importantly, additive manufacturing is inherently slower than conventional manufacturing processes, since parts are built one at a time. This means that AM in general cannot compete with traditional methods for large scale manufacturing. Another problem facing AM has to do with the resolution of printed lines, often limited to minimum width of  $\sim 100\text{ }\mu\text{m}$ . This leads to parts with much higher surface roughness compared to injection molded or milled plastics. Furthermore, the accuracy of printed parts can deviate significantly with respect to their computer drafted models due to instabilities in the printing process and because of post-deposition cooling and/or shrinkage that result from complex cure processes. More importantly, the layer-by-layer approach that is used in most AM methods can generate ‘weak links’ between lines, which may result in significant loss of overall mechanical properties such as toughness. This also leads to difficulty in predicting the mechanical properties of 3D printed parts since the strength of the material is intimately related to the printing parameters (i.e. print direction and any cure on demand features).

Advances in both printing methodologies and new classes of printable materials are needed in order to overcome the aforementioned challenges. These two developments require a synergistic approach since each material requires specific considerations for printing methodology. The following sections will describe the various printing methods that are available for additive manufacturing of polymer materials and provide a basic review of each

method with respect to advantages and disadvantages, compatible materials, cure chemistries, material properties, and opportunities in new material development.

## 2. PRINTING METHODS

### 2.1. Fused-Deposition Modelling

Fused deposition modelling (FDM) is the process of printing structures in a layer-by-layer fashion via extrusion of a polymer filament through a heated nozzle, generally conducted by using simple non-reactive thermoplastics. A 3-dimensional structure is first drafted in CAD and then deconstructed into a series of 2D slices, which are printed layer-by-layer via the movement of the extrusion nozzle in the x-y plane (Figure 1). The build platform (or the extrusion nozzle) moves along the z-axis in order to allow the nozzle to print multiple layers sequentially. The melted polymer undergoes thermal fusion with the underlying structure and solidifies upon cooling to form a permanently bonded structure. Support materials are printed from a second nozzle when overhangs and bridges are needed, since the molten polymer will collapse in the absence of an underlying structure to rest on. Support materials can be removed after the printing is completed either by mechanical agitation or by selective dissolution of the support.

Fused deposition modelling is the least expensive and most user friendly 3D printing technique, as the printing hardware uses a relatively small number of working parts and the thermoplastic materials are often commodity plastics which are environmentally and mechanically stable. Compared to other printing techniques, FDM allows for greater freedom in choice of materials since there are no chemical reactions taking place during the print process. The only requirement for FDM is that the material be a thermoplastic with melt and solidification temperatures that are accessible using the printing hardware.

Compared to other AM techniques, parts printed by FDM are more suitable for demanding applications where high strength and thermal resistance is necessary, since the wide range of thermoplastics that are amenable to FDM encompasses materials with good mechanical properties. FDM printed parts are most commonly used as structural prototypes, but can also be used in some cases for end-use mechanical parts. The most commonly used material in commercial FDM printers is ABS (acrylonitrile butadiene styrene copolymer) due to its low cost and durability; however, a number of other traditional thermoplastics are commercially available for FDM. For example, Table 1 provides a list of materials that are available for use on the Fortus model printers from Stratasys Ltd. and their corresponding mechanical properties. It represents the majority of commercially available materials for FDM, though other commonly employed thermoplastics for FDM include biocompatible polylactide (PLA), poly(lactic-co-glycolic acid), and polycaprolactone (PCL), which are commonly utilized for tissue scaffolds.

Table 2 shows the bulk mechanical properties of some of the same polymers in order to provide a comparison. Comparing the bulk mechanical properties to those of FDM printed parts reveals that printed parts generally have lower performance compared to the bulk material (bulk properties presented in Table 2 represent average values that have been calculated from over 50 reports). This is expected, since the thermal fusion bonding process that occurs during FDM leads to parts with relatively weak connections between layers, and generates a final structure with internal porosity. In some cases the difference in mechanical properties is very large,

particularly for maximum elongation at break. For example, the tensile strength of FDM printed Nylon 12 (48 MPa) is only 60% of value for the bulk material (80 MPa). Likewise, the impact strength of bulk polycarbonate is more than ten times greater than that of the FDM printed polycarbonate. For the most part the polymers maintain the same rank in mechanical properties regardless of whether they are printed or measured in bulk. Thus, while the FDM process generally leads to weaker structures compared to bulk-processing, the intrinsic properties of the polymer are still the limiting factor affecting the overall strength of printed structures.

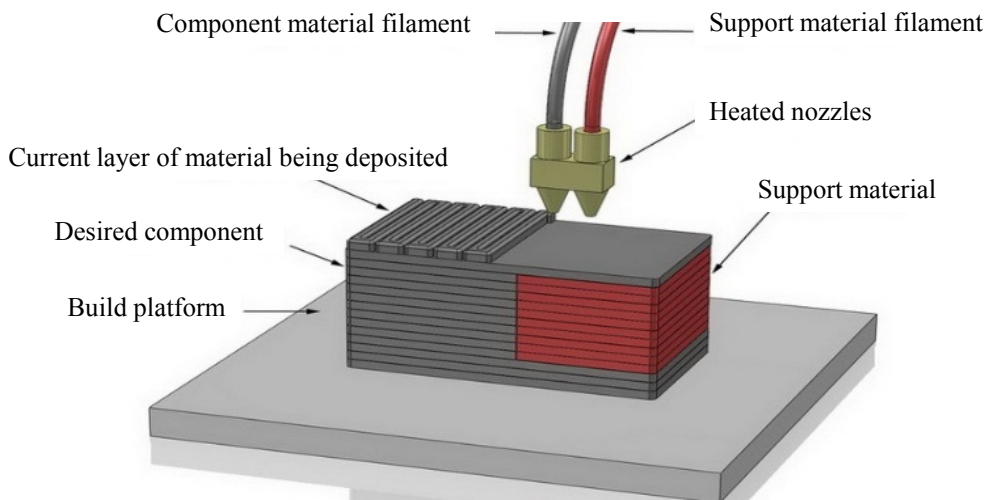


**Figure 1. Illustration of FDM process (<http://www.slideshare.net/johnbrittas/rapid-prototyping-technologiesapplications-part-deposition-planning-2>).**

It is important to recognize that structures fabricated using FDM are also heterogeneous in regards to the printed filament geometry, which in turn leads to heterogeneous or anisotropic mechanical properties. The choice of print direction is therefore critical for achieving optimal performance of parts printed using FDM. The values presented in Table 1 correspond to the maximum value when more than one print direction was tested. The data suggests that generally all of the mechanical properties will be simultaneously optimized for a particular print direction.

Several studies have focused on improving the strength of FDM printed structures by using alternative or modified materials. Carbon fiber reinforced ABS composites have demonstrated improved tensile strength at low fiber loadings (~5-10%), but with a general loss in ductility and toughness.<sup>10</sup> Brittleness of the composites has been attributed to poor bonding between the fiber/matrix.<sup>10a</sup> More recently, the German company INDMATEC has developed a polyether ether ketone (PEEK) filament and FDM printing hardware that can operate at the high temperatures required to process PEEK (m.p. = 343 °C). The high strength of PEEK along with its chemical and abrasion resistance opens new doors for applications of FDM printed structures in aerospace, automotive, and electronics sectors.

One major challenge with FDM is printing elastomeric structures. This is due in part to the weak interlayer connections that arise from thermal fusion during printing, which cannot

accommodate large strains. This is clear when comparing the elongation at break for printed parts (Table 1) vs. bulk properties (Table 2). In addition, high performance elastomers are generally achieved with vulcanized materials that possess heavily crosslinked covalent network points. Printing highly elastic structures is a challenge using thermoplastic polymers. To date, only moderate elasticity has been achieved with FDM printed parts (i.e. PCL structures), leaving a large gap to be filled for achievable FDM material properties.

Aside from mechanical applications of printed structures there has also been a growing interest in applying FDM printing to functional materials. For example, researchers have managed to print conductive PCL structures by incorporating carbon black as filler (15 wt% loading), demonstrating low surface resistance of  $\sim 0.1$  ohm m for use in flexible sensors.<sup>11</sup> Higher loading of carbon fillers can be limited by a significant loss in ductility of the material.<sup>12</sup> Meanwhile, conductive polymers have not yet been applied to FDM due to their difficult processing; however, with judicious choice of polyaniline dopant materials it is possible to prepare conductive polyaniline (PAni-DBSA) that can be melt-blended with poly(vinylidene fluoride) (PVDF) and/or poly(methyl methacrylate) PMMA at 200 °C.<sup>13</sup> Although there has been some discrepancy in the literature regarding the conductivity of PAni-DBSA (0.03 S/cm – 2 S/cm),<sup>13,14</sup> these materials are of interest for printing conductive 3D structures, since PAni-DBSA can be blended with thermoplastics at loadings as high as 50% while maintaining robust mechanical properties.

The ease of FDM makes this technique particularly attractive for explorative research on new printable materials. For this reason, recent developments in FDM have shifted to printing functional materials with properties that go beyond those of traditional thermoplastics (*vide infra*, Section 3.7). However, FDM printed structures would greatly benefit from new approaches that improve interlayer fusion and reduce the overall anisotropy of properties.

**Table 1. Mechanical properties of FDM printed thermoplastics**

Material	Tensile Strength Ultimate (MPa)	Elongation at Break	Flexural Strength (MPa)	IZOD Impact notched (J/m)
Acrylonitrile-Butadiene-Styrene (ABS)	33	6 %	58 MPa	106
Polycarbonate (PC)	57	5 %	89 MPa	73
Polycarbonate-ABS blend (PC-ABS)	34	5 %	59 MPa	235
ABS-ESD7	36	3 %	61 MPa	28
Acrylonitrile-Styrene-Acrylate (ASA)	34	9 %	59 MPa	64
Nylon 12	46	30 %	67 MPa	135
ULTEM™ 9085 <sup>a</sup>	69	6 %	112 MPa	120
ULTEM™ 1010 <sup>a</sup>	81	3 %	144 MPa	41
Polyphenylsulfone (PPSF)	55	3 %	110 MPa	59

Data obtained from <http://www.stratasys.com/>. Maximum values are reported for properties that were measured for more than one print direction. <sup>a</sup>Ultem products are polyetherimide based.

**Table 2. Bulk mechanical properties of selected thermoplastics<sup>15</sup>**

Material	Tensile Strength Ultimate (MPa)	Elongation at Break	Flexural Strength (MPa)	IZOD Impact notched (J/m)
ABS (extruded)	38 MPa	34 %	64 MPa	326 J/m
PC (extruded)	68 MPa	83 %	89 MPa	670 J/m
Nylon 12	80 MPa	54 %	114 MPa	223 J/m
ULTEM™ 1010 <sup>a</sup>	110 MPa	60 %	165 MPa	32 J/m

<sup>a</sup>Ultem products are polyetherimide based.

## 2.2. Stereolithography

The AM technique known as stereolithography (SLA) works by irradiating the surface of a liquid photopolymer resin with UV light in order to cure 2-dimensional layers sequentially. An underlying platform is used to support the structure during layer formation, and presents the initial surface for the first photopolymerized layer. After each layer is cured, the platform is lowered by a distance equal to the layer thickness, and the liquid resin is repeatedly allowed to coat the surface of the build structure. Sequential layers are then photopolymerized on top of the structure, with programmed 2-dimensional patterns that ultimately define the features of the fabricated 3D component. Un-polymerized resin is washed away from the solidified product after printing has finished.

Stereolithography printers are more expensive than FDM printers and are considered less user-friendly. For this reason they are less common for hobbyists and for ‘desktop’ printing. Stereolithography is also generally a slower process than FDM, and therefore it is often not a practical technique for printing large objects. On the other hand, SLA has the advantage of being able to print high resolution parts, with layer thickness of  $\sim 20 \mu\text{m}$ . The surface roughness and final appearance of SLA printed parts are generally much better than those made by FDM, and the accuracy of parts with respect to CAD models is improved.

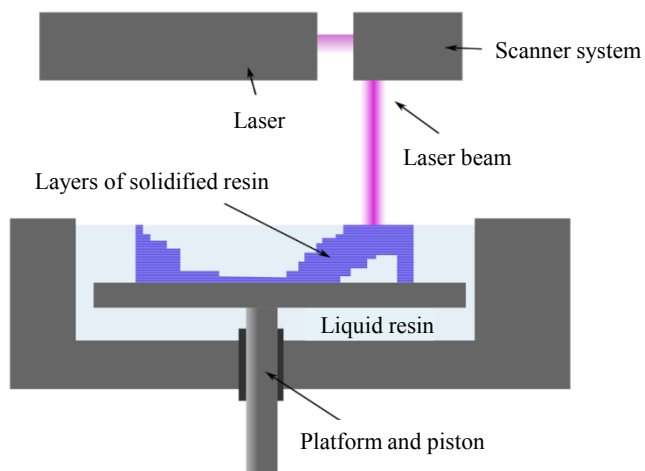


**Figure 2. Illustration of stereolithography process**  
[\(https://en.wikipedia.org/wiki/Stereolithography#/media/File:Stereolithography\\_apparatus\\_vector.svg\)](https://en.wikipedia.org/wiki/Stereolithography#/media/File:Stereolithography_apparatus_vector.svg)

Compared to FDM there are greater restrictions on the types of resins and final polymer structures attainable via stereolithography since a key requirement for these resins is fast photoinitiated cure, commonly achieved with free radical polymerization reactions. SLA resins must also have fine-tuned viscosity in order to facilitate fast coating of the build surface and produce smooth, stable liquid surfaces. These requirements have limited SLA resins to acrylates, vinyl ether, and epoxide containing monomers. Figure 3 shows a collection of common monomers, reactive diluents, and photoinitiators used with SLA. Common acrylate monomers can be small molecules, oligomers, or polymers with multiple reactive groups that are capable of fast cross-linking.<sup>16</sup> High reactivity is critical for SLA monomers, since photopolymerization must occur rapidly in order to print structures in a reasonable amount of time. Complete conversion of monomers is almost never achieved during the SLA printing process, and most parts require post-print UV cure, typically for 60-90 minutes. Other common SLA monomers include vinyl ethers and epoxides, which are typically cured via cationic polymerization initiated by a photoacid generator.

The mechanical properties of SLA-printed parts from some commercial resins are given in Table 3. The SLA process involves covalent bond formation between the build structure and the newly polymerized layer, and therefore printed parts are expected to behave more like their bulk counterparts. This is likely facilitated by the fact that the monomer may act as a solvent and allow for penetration of monomer into the previous layer. In addition, some unreacted monomer groups are expected to remain on a cured surface. However, this is difficult to assess from the literature since bulk properties of SLA resins are not commonly reported. In general, elongation at break for SLA parts is significantly larger than for FDM parts due to the more flexible monomers that are amenable to stereolithography. On the other hand, SLA polymers have a relatively small variation in their mechanical properties, and do not match the strength of FDM materials. They are mostly glassy amorphous materials with brittle fracture tendencies that cannot be compared with, for example, ABS or Nylon.

**Table 3. Mechanical properties of commercially available SLA materials**

Material	Tensile Strength Ultimate (MPa)	Elongation at Break	Flexural Strength (MPa)	IZOD Impact notched (J/m)
Watershed 11110	48	25 %	64	19
Waterclear	43	37 %	58	45
Nanotool (filled resin)	78	1 %	121	15
DMX-SL	45	28%	68	71
Somos 9110 (epoxy)	31	21%	44	55
SL 5170	60	8 %	108	37

Data obtained from [http://www.rpsupport.co.uk/materials/materials\\_stereolithography.html](http://www.rpsupport.co.uk/materials/materials_stereolithography.html). Maximum values are reported for properties that were measured for more than one print direction.

### 2.3. Direct-Write

Direct-write generally refers to the method of printing liquid resin inks that undergo rapid polymerization upon deposition, most often by an immediate UV curing (Figure 4). The process

is similar to FDM in that a moving nozzle is used to draw 2-dimensional layers one on top of the other; however, unlike FDM which employs a simple thermal extrusion of a thermoplastic, direct-write processes normally involve a chemical reaction which allows for on-demand chemically driven solidification (cure process) during deposition. Direct-write is also used to describe the process of printing viscous inks that undergo transformation to a self-supporting gel during deposition with perhaps secondary cure initiated after the part has been manufactured. In some cases post-print thermal or UV cures are used to further solidify the printed structures.

Direct-write is currently one of the most versatile additive manufacturing techniques and undergoing rapid innovation, capable of printing structures with complex materials gradients, since multiple resin reservoirs can be utilized during printing. Resin mixing during printing enables fine-tuned polymer compositions and can be used for spatial control of the thermomechanical properties of the printed structure or the design of materials with property gradients. Furthermore, UV cured resins maintain the attractive bulk-like characteristics that result from covalent bond formation during printing. The mechanical properties of direct-write polymers available for Stratasys printers (acrylate based resins) are given in Table 4. The direct-write materials generally exhibit similar properties as SLA resins, with relatively large elongation at break and poor impact strength. A rubber-like resin available from Stratasys provides unique elastomeric properties, with very low tensile modulus and an elongation at break exceeding 200%.

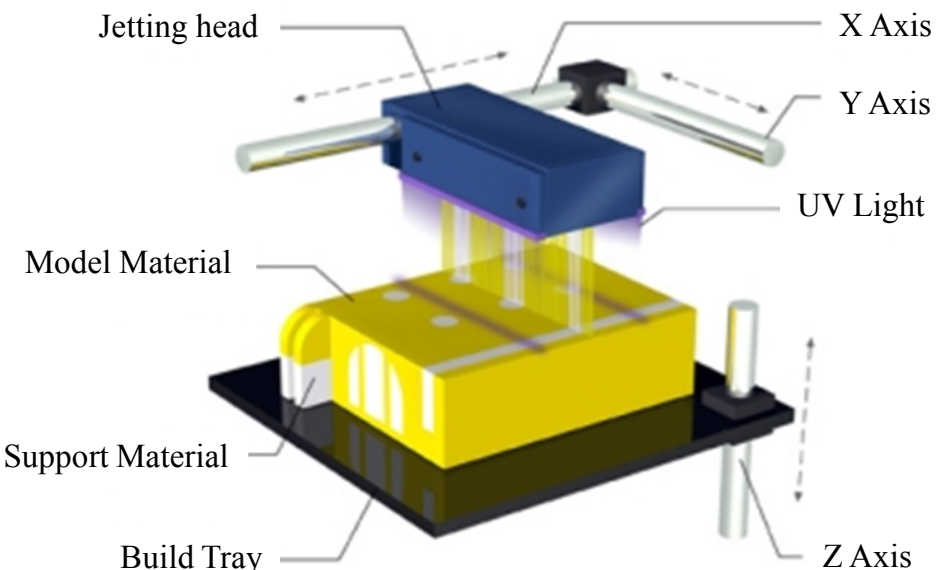


**Figure 3. Illustration of the direct-write printing process (<http://proto3000.com/polyjet-3d-printing-services-process.php>)**

It should be emphasized that direct-write resins can generally be mixed at arbitrary ratios to provide a large variety of properties. This feature has recently been utilized to construct 3D materials with specific segments that exhibit shape memory behavior, with glass transition temperatures that can be controlled via resin composition. By varying the glass transition

temperature of different actuating components, discrete folding events can be triggered at different temperatures. This approach has enabled new structures termed ‘4D materials’, which can undergo controlled self-folding from a temporary shape (with programmed stress) to a permanent shape via activation by external stimuli such as heat.<sup>17</sup>

The photoinitiated polymerization process in direct-write is analogous to that which occurs in SLA, and thus photocured (mostly free radical) direct-write resins are bound by the same constraints, e.g. fast kinetics, high conversion upon reaction, long pot-life. On the other hand, direct-write of shear-thinning viscous pre-polymer structures followed by a post-deposition cure can overcome these requirements. For example, 3D printed silicone thermoset elastomers have been fabricated at Sandia and LLNL<sup>18</sup> by printing a highly viscous (~ 610,000 cP) silicon resin which is able to maintain structural integrity until a post deposition bake. The especially high viscosity of this resin, controlled by a thixotropic additive, enables the pre-cured structure to maintain its deposition shape and allows for the fabrication of even porous structures with exceptional elastic behavior after thermal curing. This method allows for greater freedom in materials properties, since the cross-link density can be tuned independent of the deposition behavior and the cross-linking reactions are not confined to rapid photoinitiated polymerizations. However, to date this method has been mainly limited to reactive high viscosity silicone resins.

Direct-write has also been utilized for printing hydrogels, materials that find many applications in the biomedical arena. Hydrogels with physical cross-links (i.e. hydrogen bonds or ionic interactions) can be printed by thermal extrusion analogous to FDM, where a gelation temperature is traversed during the printing process, leading to coagulation of the network. Direct-writing of hydrogels may also be achieved by printing polyelectrolyte inks into a hydrophobic solvent reservoir which leads to fast coagulation due to increased ionic interactions.

**Table 4. Mechanical properties of commercially available direct-write materials**

Material	Tensile Strength Ultimate (MPa)	Elongation at Break	Flexural Strength (MPa)	IZOD Impact notched (J/m)
‘Digital ABS’	60	40 %	75	80
High Temp Material (RGD525)	80	15 %	130	16
Transparent Material (RGD720)	65	25 %	110	30
Rigid Opaque Material (RGD840)	60	25%	70	30
Simulated Polypropylene (RGD430)	30	50%	40	50
Rubber-like Material (FLX930/FLX980)	1.5	220 %	-	-

Data obtained from <http://www.stratasys.com/materials/polyjet/digital-abs>.

Using this method, researchers were able to deposit 3-dimensional structures with line widths of ~ 1 µm and, and surface charge that could be controlled by varying the stoichiometry of anion/cation in the polyelectrolyte blends.<sup>19</sup>

Similar to stereolithography, chemical reactions that are useful for direct-write are limited to those with rapid kinetics and which produce little or no byproducts. Commercially successful direct-write materials are essentially limited to acrylates systems or perhaps some evolving cationically photo-cured epoxy resins. The attractive compositional control of direct-write would further benefit from new reactions that allow for desirable mechanical properties, such as high-strength materials. In addition, the materials landscape is wide open for developing self-supporting ink systems that undergo curing in a second, post-print stage. This route opens new doors for cross-linking chemistry and removes the typical restrictions on polymer resins that can be considered for additive manufacturing.

## 2.4. Continuous Liquid Interface Production

Continuous Liquid Interface Production (CLIP) is a method that was recently developed by researchers at the University of North Carolina at Chapel Hill in order to overcome the long fabrication times of other additive manufacturing techniques.<sup>20</sup> The method utilizes a UV curable resin similar to stereolithography, except the resin is illuminated from the bottom while the build platform continuously rises out of the resin bed, creating parts in a continuous fashion without defined layers (Figure 5). The essential component of this technology that enables continuous processing is a transparent oxygen permeable fluoropolymer film, which acts as the base of the photopolymer resin reservoir. This leads to a ‘dead zone’ at the interface between the liquid resin and the oxygen permeable membrane where photopolymerization is inhibited due to oxygen. This is a critical feature of the design as it prevents the resin from attaching to the underlying window, and thus allows for continuous polymerization of parts at a much faster rate than FDM, stereolithography, or direct-write. Carbon3D, the company that is developing CLIP printers, claims that the CLIP process is 25-100 times faster than stereolithography or direct-write. Parts which would take more than a few hours to print by traditional additive manufacturing approaches can be finished in less than ten minutes using CLIP.

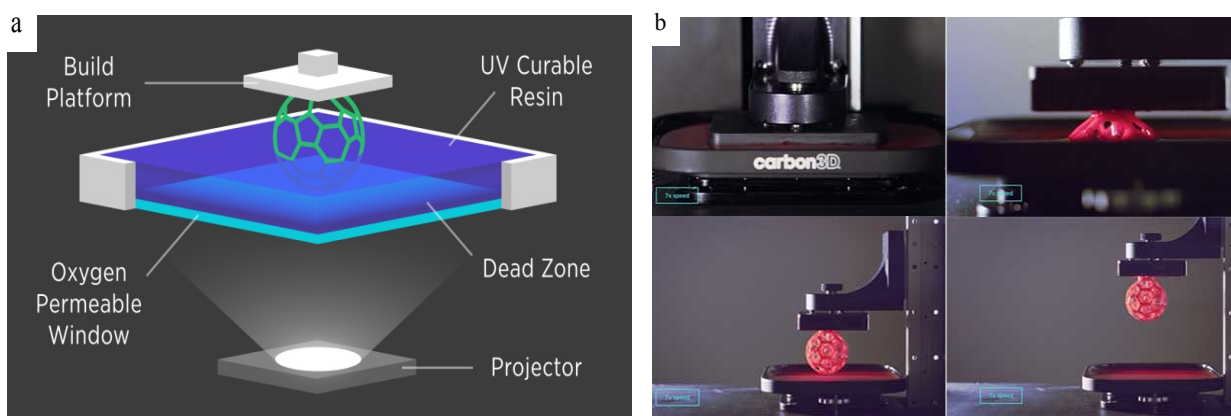


**Figure 4. (a) Illustration of CLIP components and printing technique. (b) Photographs of CLIP printer and printed component. ([www.carbon3D.com](http://www.carbon3D.com))**

Researchers have reported that CLIP can be used to fabricate parts from elastomers, tough polymers, and biomaterials.<sup>19</sup> Resins for CLIP are limited to those that undergo radical addition

polymerization and are inhibited by oxygen. Acid catalyzed cationic polymerizations of epoxide or vinyl ether monomers are not compatible with the CLIP process, and therefore the materials set available for CLIP printing is limited. However, other researches are pursuing continuous printing methods that work by illuminating the top of resin beds and do not require oxygen sensitive reactions in order to function.<sup>21</sup>

## 2.5. Selective Laser Sintering

Selective laser sintering (SLS) is a technique which utilizes a powder bed of solid thermoplastic particles that are processed into layered structures via localized melting/crystallization by heating using a CO<sub>2</sub> laser.<sup>22</sup> Irradiation of the powder surface with the infrared laser leads to rapid heating which sinters the powder due to complete or partial melting, followed by recrystallization (Figure 6). After a 2-dimensional layer is sintered, the build platform is lowered a distance equal to the height of one layer, and a fresh layer of powder is spread over top of the object. Sequential layer-by-layer sintering leads to the fabrication of 3-dimensional objects. Selective laser sintering printers are more expensive than FDM, SLA, and direct write printers, and therefore SLS is rarely used for ‘desktop’ projects. On the other hand, SLS can process plastics with high melting points and thus can produce tough parts that are not easily accessible by FDM.

In order to print high-quality parts using SLS, controlled sintering must occur only where the laser irradiates the polymer bed, e.g. diffuse melting due to heat transfer should be limited. This is best achieved when thermoplastics with large heats of fusion and sharp transitions in

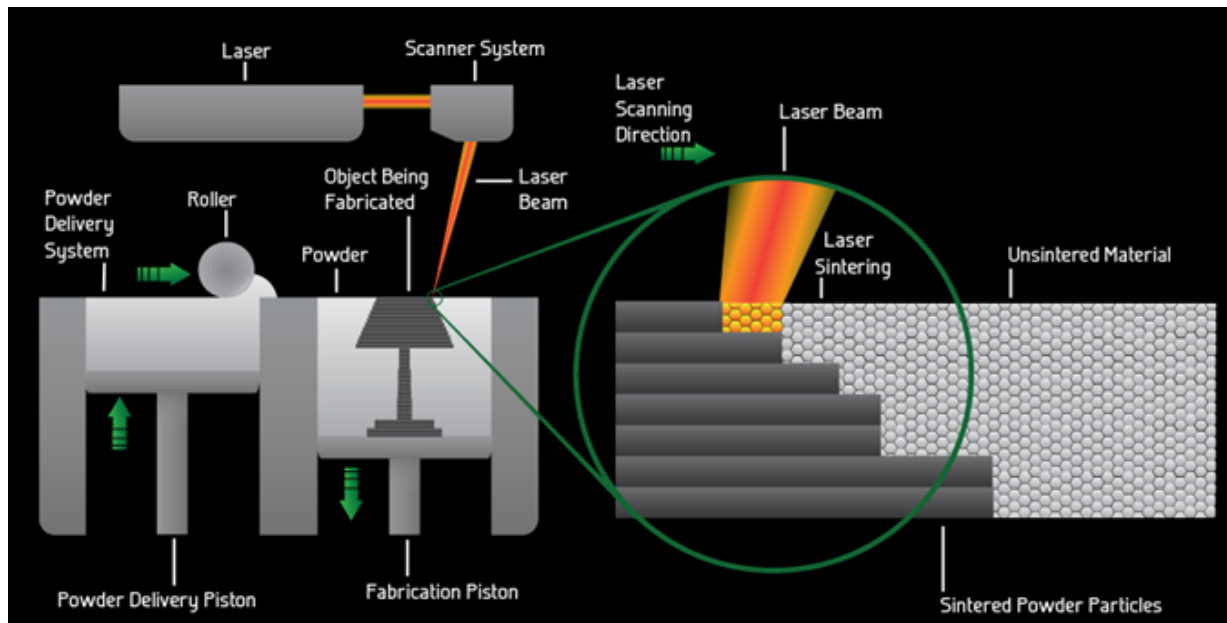


**Figure 5. Illustration of the selective laser sintering process**  
(<http://rapidprototypingservicescanada.com>)

viscosity are employed. In addition, SLS thermoplastics should ideally possess narrow thermal transitions in order to promote fast melting/crystallization. Therefore, SLS is more commonly used for printing semi-crystalline structures. However, semi-crystalline polymers exhibit a large and rapid shrinkage upon crystallization which can lead to geometrical inaccuracies and internal stress during printing. This problem is overcome by using amorphous thermoplastics, and thus there is a trade off in using semi-crystalline vs. amorphous materials. Amorphous polymers that have been successfully printed using SLS include polycarbonate and polystyrene. Notably, SLS has been used to print structures from the engineering plastics PEEK and polyether ketone ketone (PEKK) which possess high chemical resistance, heat resistance, and the ability to withstand high mechanical loads. These plastics are not amenable to most FDM printers due to their very high melting points and higher processing viscosity. For any of these high temperature sintering processes, the beginning of polymer degradation under oxidative environments or thermally induced decomposition reactions could be a concern. But if conditions can be kept within the range of usual processing temperatures (extrusion or injection molding) such effects should be controllable.

3D Systems currently offers commercial SLS printers with seven different thermoplastic resins, including a styrene based thermoplastic, a rubber-like elastomer, and a fiber reinforced composite. Often times, SLS parts are infiltrated with a secondary resin after printing, in order to fill in the highly porous structures that result from the sintering process.

### 3. THE CHEMISTRY OF ADDITIVE MANUFACTURING: OLD AND NEW

#### 3.1. Monomers

Resin formulations for additive manufacturing require careful consideration of monomer structures in order to achieve desired properties of the manufactured part. The most common monomers found in stereolithography and direct-write resins are shown in Figure 6. Acrylate monomers are the most commonly used for additive manufacturing (i.e. Stratasys and Formlabs resins) due to their fast polymerization kinetics and wide range of molecular structures. Monomers **5-7** with only one acrylate (or vinyl) group are considered reactive diluents. These compounds have low viscosity and are often employed to modify the resin rheology.

The molecular structures of monomers are critical in determining the thermomechanical properties of the printed parts, since the monomer structure defines the flexibility of network segments, the solid-state structure (amorphous vs. crystalline), and the crosslink density. Desired mechanical properties can therefore be tuned by careful choice of the monomers used in the polymer resin. For example, the polymer  $T_g$  can be increased by incorporating monomers with reduced chain mobility or by increasing the crosslink density. A resin that incorporates a large percentage of the branched monomer **2** would lead to a comparatively high crosslink density due

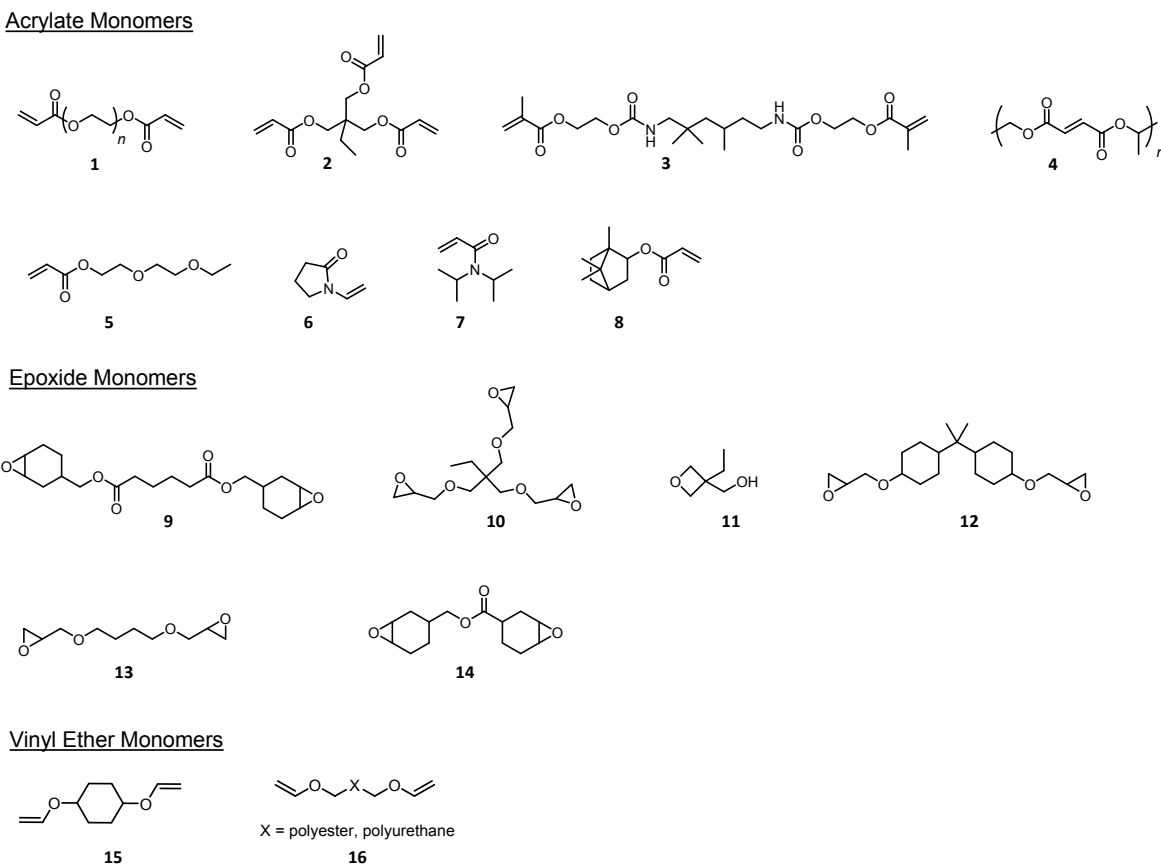


**Figure 6. Common monomers used in stereolithography and direct-write resins**

to the tri-functionality (three acrylate groups), and would thereby afford a material with high  $T_g$ . These considerations impact the formulation of resins with desirable mechanical properties. As of yet there are no commercial 3D printers that utilize vinyl ether based resins. However, Lapin et al. have disclosed stereolithography resins that incorporate both epoxide and vinyl ether monomers.<sup>23</sup>

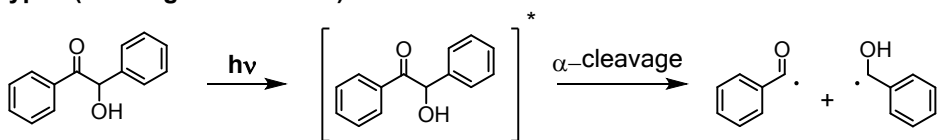
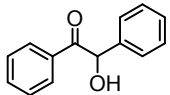
### 3.2. Radical Photoinitiators

Radical photoinitiators can be classified as either type I or type II depending on their mechanism of initiation.<sup>24</sup> Under illumination (UV irradiation), type I photoinitiators undergo bond cleavage from the triple excited state, resulting in two unique radical species (Figure 7). Typically, one of the radical species is more reactive and acts as the major initiator for polymerization. Type II photoinitiators require a hydrogen donor co-catalyst, as the mechanism relies on excited state hydrogen abstraction to form a reactive radical species on the hydrogen donor. Examples of the many type I and type II radical photoinitiators that are commercially available (Sigma-Aldrich, BASF, ESSTECH Inc.) are shown in Figure 7.

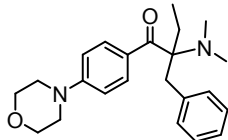
The choice of radical photoinitiator depends on the particular application. In general, type I initiators are more reactive than type II initiators since the kinetics of radical formation are first order with respect to the initiator and depend only on the concentration of a single species. Benzoin initiators are particularly reactive since they are hardly affected by triplet quenchers such as styrene, and are therefore useful for initiating less reactive monomers. However, the high reactivity of benzoin initiators limits the pot life of resin formulations and benzoin initiators are not ideal for processes that require long-term stability. Benzyl ketals have greater stability than benzoin initiators and, like type II acetophenone initiators, benzyl ketals develop little coloration over time and are important for colorless resin formulations. Aminoalkyl phenone and acylphosphine oxide initiators possess longer wavelength absorption and are ideal for resins with limited UV transparency, such as those that incorporate  $TiO_2$  as filler. All of the resins available for Stratasys direct-write printers are based on acrylic monomers and acylphosphine oxide initiators.

An important consideration for type II initiators is the choice of hydrogen donor co-catalyst, since hydrogen abstraction must out-compete side reactions during the initiation step. Tertiary amines are the most common hydrogen donors due to their greater reactivity as compared to alcohols and ethers. The volatility and odor of small molecule amines can be problematic in some cases, and this can be circumvented by using polymer hydrogen donors such as polyethylene imine. In addition, some thioxanthone type II initiators have been synthesized which incorporate hydrogen donor functionality, such as thiol group, directly into the thioxanthone structure, alleviating the need for a co-catalyst.<sup>25</sup>

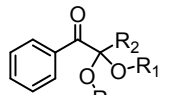
In addition to the typical radical photoinitiators for acrylate polymerizations, photoinitiators with two-photon absorption (2PA) have also been pursued for high-resolution stereolithography. Two-photon absorption materials can be excited by absorption of two low energy photons, typically in the near infrared, and exhibit a quadratic dependence of absorption

**Type I (Cleavage Mechanism)****Type I Photoinitiators**

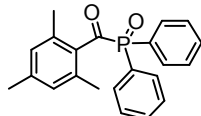
benzoin derivatives



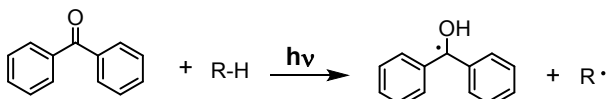
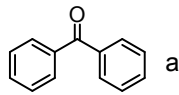
aminoalkyl phenones



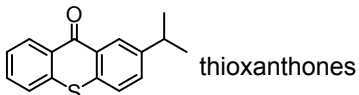
benzyl ketals



acylphosphine oxides

**Type II (Hydrogen Abstraction Mechanism)****Type II Photoinitiators**

acetophenones



thioxanthones

**Figure 7. Type I and Type II radical photoinitiators**

on laser intensity which enables a focused point of initiation and allows for printed parts with line widths between 500nm-1μm.<sup>16b,26</sup> Several 2PA initiators are commercially available from CIBA Specialty Chemicals, albeit with low efficiency.<sup>27</sup>

### 3.3. Photoacid Generators (Cationic Initiators)

Stereolithography is essentially an extension of the photolithography processes that have been used for decades in the semiconductor industry. The well-developed photoacid generators (PAGs) used in photolithography are therefore useful as photoinitiators for cationic polymerizations used in additive manufacturing. The most common commercially available PAGs are shown in Figure 8, along with their photodecomposition products. They can be categorized as either ionic PAGs or non-ionic PAGs. The most common ionic PAGs are the diaryl iodoniums and triaryl sulfoniums, though aryl diazoniums and triaryl phosphoniums are also used. Ionic PAGs possess good thermal stability and tunable absorption that depends on aryl substitution. One potential drawback of the ionic PAGs is their limited solubility in organic

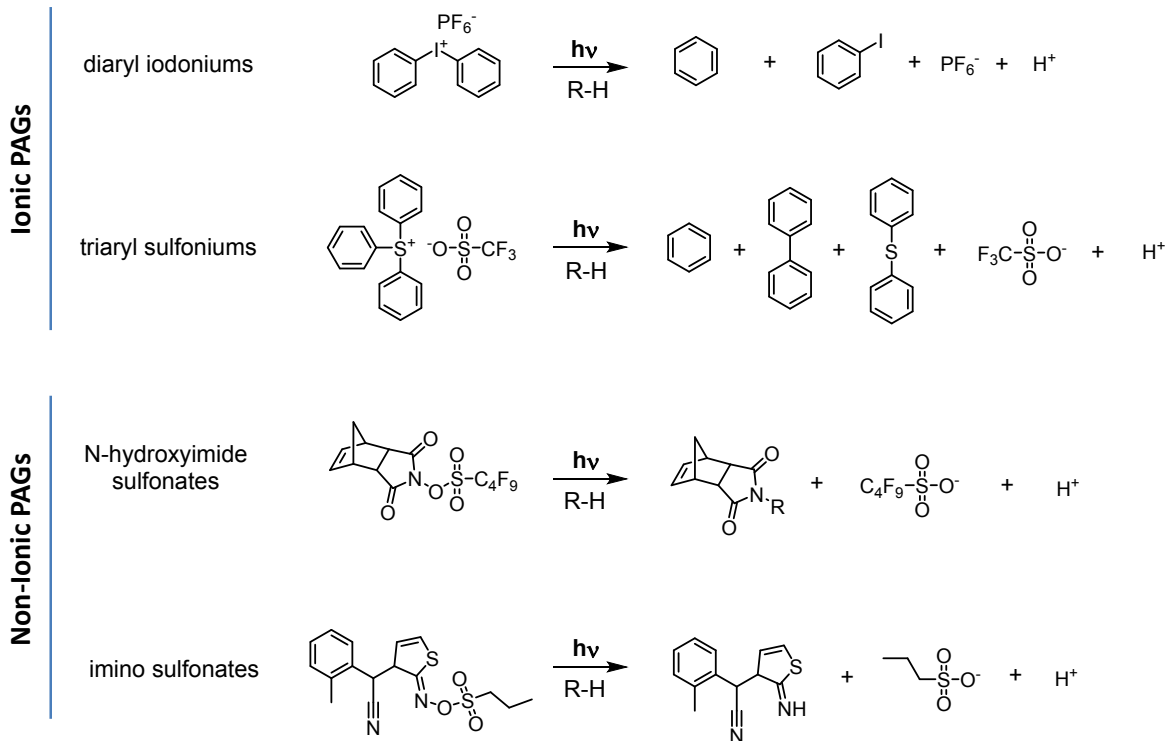


**Figure 8. Commercially available PAGs and their photodecomposition products**

solvents. However, this can be solved by structural modifications to the aryl substituents. 3D Systems uses mixed triaryl sulfonium PAGs in order to photopolymerize the epoxy resins used with their stereolithography printers. The 3D Systems epoxy resins are generally mixtures of monomers **9-14** (Figure 6).

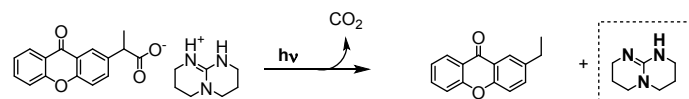
The most common non-ionic PAGs are sulfonate compounds that possess a weak N-O bond, which cleaves to eventually produce the sulfonic acid. In general, non-ionic PAGS have better solubility in organic solvents compared to ionic PAGs, but with lower thermal stability. It is important to note that both the ionic and non-ionic PAGs generate acid via radical intermediates that undergo hydrogen abstraction reactions with either solvent or monomer. This leads to unwanted byproducts via radical coupling or free radical polymerization.

A few examples of two-photon photoacid generators can also be found in the literature. By incorporating sulfonium groups into electron rich compounds with extended  $\pi$ -conjugation, two-photon acid generation has been possible with near IR wavelengths  $\sim 800$  nm.<sup>28</sup>

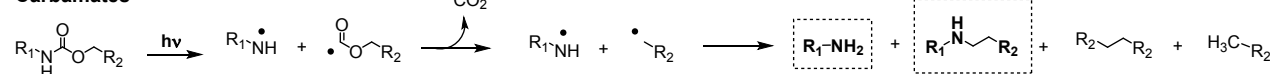
### 3.4. Photobase Generators

Photobase generators (PBGs) are attractive initiators for epoxide polymerization as they do not corrode metal substrates, a problem that plagues most PAGs. On the other hand, the chemistry of PBGs is less developed compared to PAGs and only a few PBGs have been successfully used as catalysts for epoxy polymerization (Figure 9). Most PBGs liberate amine

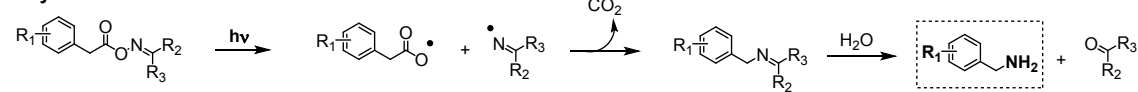
**Ammonium Salts**



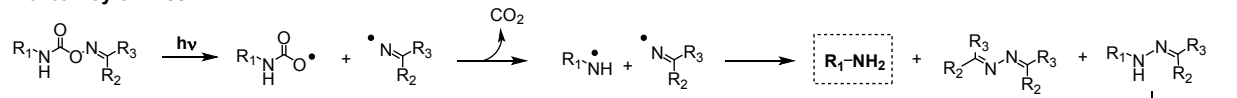
**Carbamates**



**Acyloximes**



**Carbamoyloximes**



**Amidines**

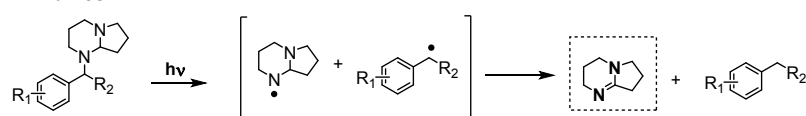


**Figure 9. Amine photobase generators**

bases, which act to initiate epoxide polymerization either through nucleophilic attack, or via deprotonation of a separate species to activate a nucleophile. In general, the nucleophilicity of PBG amines is too low for them to be used as initiators at room temperature. Meanwhile, many PBGs will decompose into reactive amine groups at high temperatures even in the absence of light. Thus, PBGs are generally most effective in a small temperature window, where there is enough heat to provide fast polymerization kinetics, but not enough heat to decompose the PBG in the absence of light.

Ammonium salt PBGs based on the strong base triazabicyclo[4.4.0]dec-5-ene (TBD) have been developed by Arimitsu et al., where photoexcitation leads to charge transfer from the carboxylate anion to the ammonium cation, followed by loss of CO<sub>2</sub> and the formation of the neutral TBD base.<sup>29</sup> The 2-(9-Oxoxanthen-2-yl)propionic acid 1,5,7-triazabicyclo[4.4.0]dec-5-ene salt shown in Figure 9 is commercially available through TCI Chemicals (1g = \$287).

Irradiation of carbamates leads to the formation of primary and secondary amines via homolytic cleavage of the nitrogen-acyl bond, followed by loss of CO<sub>2</sub> and hydrogen abstraction or radical coupling.<sup>30</sup> Acyloximes have also been used as PBGs, which afford primary amines via hydrolysis of imine intermediates that are formed from photo-induced homolytic cleavage of the nitrogen-oxygen bond followed by loss of CO<sub>2</sub> and radical coupling. Carbamoyloximes afford primary amines and hydrazines via a similar mechanism.

Unlike the majority of PBGs which liberate  $\text{CO}_2$  along with the desired amine bases, amidine PBGs form strong bases via homolytic cleavage of the carbon-nitrogen bond followed

by hydrogen abstraction (Figure 9).<sup>31</sup> These PBGs do not generate gaseous byproducts. While the evolution of  $\text{CO}_2$  is not a problem for solution phase polymer synthesis, degassing of a neat polymer resin would likely reduce the resolution and structural integrity of additive manufactured structures. Amidine PBGs may therefore be more practical for photopolymerization of epoxy resins in AM. It should be noted that the amidine PBG precursors contain basic secondary/tertiary amines (prior to photodecomposition), and have some reactivity in their parent form which might limit the pot-life of resins incorporating amidine PBGs. However, the reactivity is greatly increased upon photodecomposition, with a jump in  $\text{p}K_b$  of 4.5 units.<sup>31</sup>

The use of photobase generators for epoxy curing has been limited due to the slow kinetics of PBG initiated epoxide polymerization. Literature examples of epoxy curing using PBGs have all relied on post-exposure baking in order to achieve more substantial conversion.<sup>32</sup> To improve the rate of PBG initiated curing several researchers have utilized epoxide-thiol resins, where liberation of basic amines catalyzes polymerization via an initial thiol deprotonation to form reactive thiolates. Two examples are shown in Figure 10 where epoxide/thiol resins were successfully cured without the need for post-exposure baking. While monomer conversion was not analyzed for the ammonium salt PBG initiated system (Figure 10, left), pencil hardness tests showed significant curing (level 3H) after 365 nm light irradiation with exposure dose of 1000  $\text{mJ}/\text{cm}^2$ . Notably, this epoxy system showed very high transparency and significantly reduced curing shrinkage compared to traditional radical UV cured resins. Similarly, the epoxide/thiol resin cured using 1,5-diaza-bicyclo[4.3.0]non-5-ene (DBN) amidine PBG (Figure 10, right) showed fast cure kinetics, with 50% monomer conversion after only  $\sim 30$  seconds irradiation at 50  $\text{mW}/\text{cm}^2$ .<sup>33</sup> These results highlight the potential for developing PBG/epoxide/thiol AM resins.

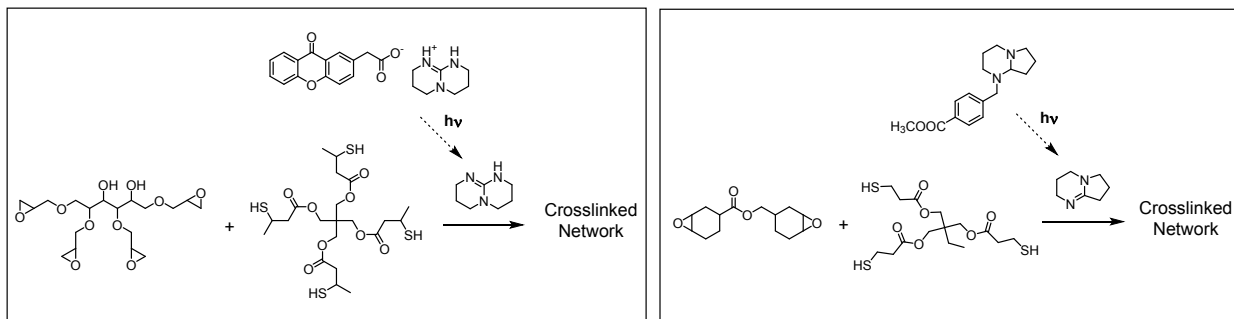


**Figure 10. Epoxy/thiol cure using ammonium salt PBG (left, Ref 32) and amidine PBG (right, Ref 36)**

### 3.5. Thermally Latent Base Catalysts

Recently, thermally latent imidazole catalysts have been developed as anionic epoxide initiators. The high reactivity of imidazole base towards epoxide ring opening has attracted

attention for some time, but the high reactivity has also led to problems with resin stability. This problem was addressed by developing a protected imidazole base that undergoes retro Michael addition at elevated temperatures to afford the free imidazole.<sup>34</sup> The decomposition temperature

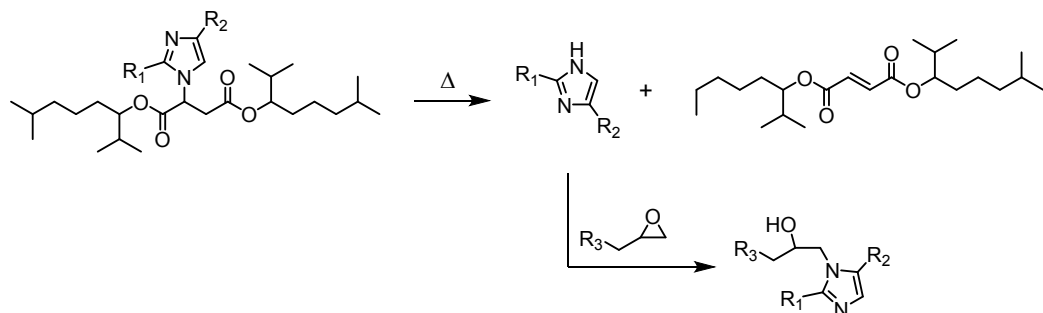


**Figure 11. Thermal decomposition of retro Michael addition latent base initiator for epoxide ring opening**

of the latent initiators was in the range of 200-250 °C. Interestingly, the decomposition temperature was lowered when the initiator was incorporated into epoxy resins. One of the latent initiators showed an onset decomposition temperature near 120 °C. Epoxy resins using the retro Michael addition latent initiators retained their liquid state after being heated at 80 °C for one hour, and could be cured upon heating to 120-150 °C. The cure kinetics for these epoxy resins were not reported however, and a relatively long cure time of 60 minutes was used which raises questions about how useful this system would be for a rapid cure resin for AM.

### 3.6. Photoclick Reactions

For photo-cure based print processes such as SLA there exists a demand for new resins with fast polymerization kinetics and tunable thermomechanical properties. In order to expand the scope of materials properties attainable via stereolithography and other photoinitiated print methods, reactions other than the common acrylate/vinyl/epoxide polymerizations are needed. In principal, any photo-activated reaction could be a candidate for SLA, though in practice it is difficult to find reactions with sufficiently fast kinetics for 3D printing that proceed cleanly with high conversion. Reactions that fall under the category of ‘click chemistry’ are especially intriguing, since these reactions are defined by fast kinetics, high conversion, minimal byproducts, and in some cases biocompatibility.<sup>35</sup> Epoxide ring-opening is often grouped into the category of click chemistry, along with a handful of other reactions that are less common in the field of polymer synthesis. The copper catalyzed alkyne-azide 1,3-dipolar cycloaddition reaction has become the mostly widely used click reaction due to its functional group tolerance, mild reaction conditions, and often quantitative yields. The alkyne-azide click reaction is catalyzed by Cu(I) and is usually carried out using a source of Cu(II), such as Cu(II) sulfate, along with a reducing agent in order to form the less stable Cu(I) species in situ. It has also been shown that the reaction can be photoinitiated either via photoinduced electron transfer from an electron rich ligand<sup>36</sup>, or by direct photoreduction Cu(II) → Cu(I) using certain Cu(II) complexes.<sup>37</sup> Adzima et al. used an acylphosphine oxide radical photoinitiator along with Cu(II) sulfate in order to promote the photoinitiated click chemistry curing of alkyne and azide functionalized

polyethylene glycol monomers.<sup>38</sup> On the other hand, the direct reduction of a Cu(II) thioxanthone carboxylate salt (Figure 12) is especially intriguing for photocure process in AM, since the reaction requires only two monomers and a single catalyst and proceeds with little to no byproducts.

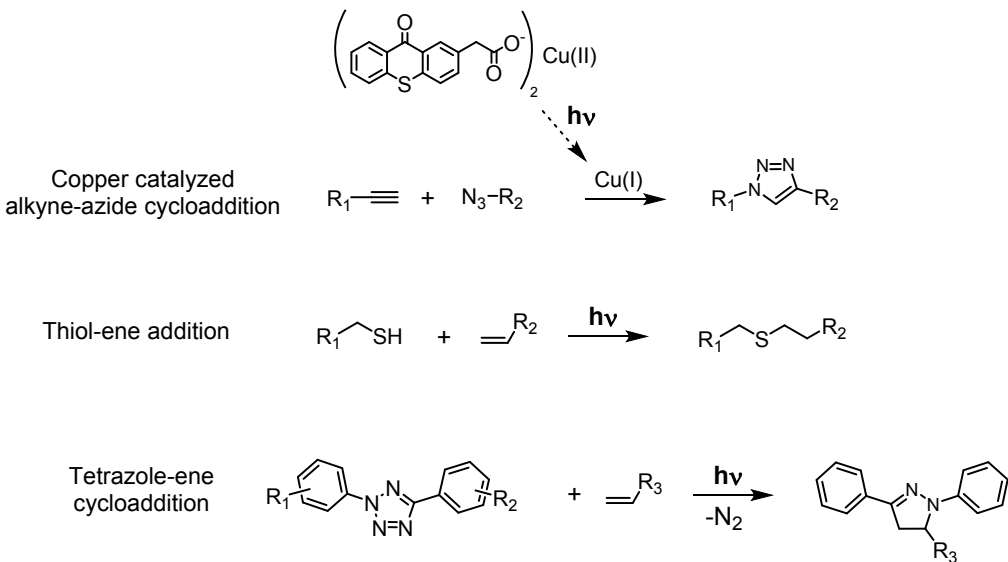


**Figure 12. Photo click reactions with potential for additive manufacturing processes**

The thiol-ene addition reaction is another ‘click chemistry’ tool that can be triggered by light.<sup>39</sup> The first report of a thiol-ene resin for 3D printing appeared recently,<sup>40</sup> demonstrating SLA printing of the novel resin without the need for initiators using direct activation of the reaction with 266 nm light or by direct two-photon absorption activation at 532 nm. Initial results show very rough surfaces of printed structures due to fibrous nature of individual voxels, which may be due to light scattering during the polymerization/nucleation. Other potential drawbacks of thiol-ene chemistry for 3D printing include the unpleasant odor of thiol monomers and the short pot-life of thiols due to disulfide formation.

The inverse-demand Diels-Alder reaction between electron rich tetrazines and electron poor olefins is another click reaction that is accelerated by light.<sup>41</sup> The fast kinetics of the tetrazole-ene cycloaddition makes this reaction attractive for 3D printing. On the other hand, stoichiometric quantities of N<sub>2</sub> gas are liberated during the reaction which would cause severe de-gassing during curing. While this would normally cause a problem with print accuracy, it may offer a unique route for direct-write approaches of foamed polymers.

### 3.7. Unusual Polymer Materials in Additive Manufacturing

In the past year there have been several exciting publications reporting unconventional polymer materials used in additive manufacturing. Functional materials have come into the spotlight for AM, including polymers that can carry out electrical functions. Cooperstein et al. recently reported conductive structures printed using stereolithography, where an oil-in-water

emulsion was first photocured followed by an extraction of the aqueous phase to form a highly porous network of polymer nanoparticles with minimal connectivity.<sup>42</sup> The porous structure was then immersed in a dispersion of silver nanoparticles which infiltrated the pores and formed a continuous conductive network (Figure 13). This approach afforded highly conductive printed structures with resistivity of  $\sim 1$  ohm·cm. Furthermore, the photopolymerization of an oil in water emulsion represents a unique way to obtain highly porous printed structures, with BET surface area as high as  $10\text{ m}^2/\text{g}$ . The surface area of the porous structures could be tuned by controlling the droplet size in the emulsion using different homogenization techniques.

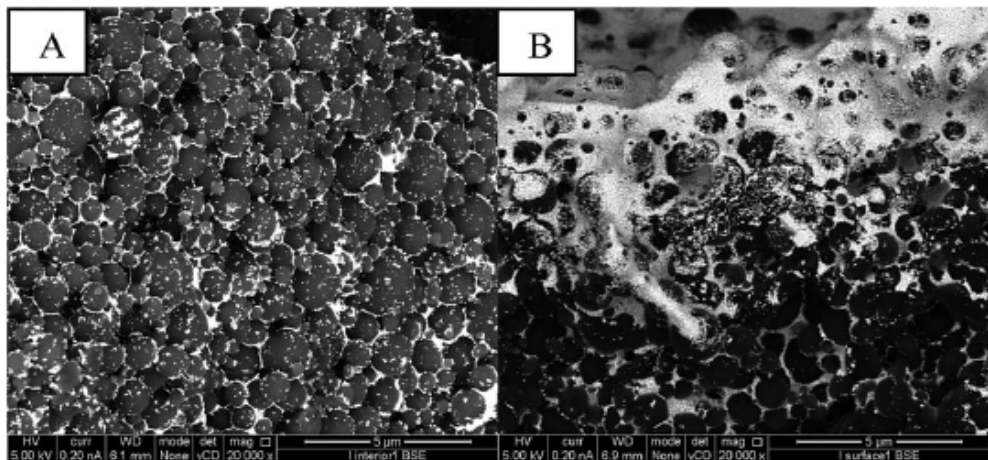


**Figure 13. SEM cross section image of printed 70% oil phase emulsion after infiltration with silver nanoparticles, showing the objects inner bulk (a) and surface (b). (Ref 41)**

3D printed piezoelectric devices have also been fabricated via an electric poling-assisted AM deposition of poly(vinylidene fluoride) (PVDF). The method was recently developed by Lee et al.<sup>43</sup> In this process, a voltage is applied between the extrusion nozzle of an FDM printer head and the build platform, which acts to orient the dipoles of the PVDF polymer (Figure 14). This method offers a significant improvement in 3D fabrication of piezoelectric devices compared to previous approaches, and alleviates the need for toxic lead components. However, the output current of the printed devices was relatively low ( $\sim 1$  nA).

Another example of an exotic polymer in AM was reported by Peterson et al., who incorporated a mechanochromic unit into the backbone of PCL in order to fabricate 3D printed structures with mechanical sensing capability.<sup>44</sup> The well-known spiropyran mechanophore was utilized, a molecule which undergoes a ring-opening reaction when a mechanical stress is applied that leads to a drastic change in color from pale yellow to deep purple (figure 15). The printed material showed similar mechanical properties as compared to commercial PCL, and could be used for visualization of mechanical stress.

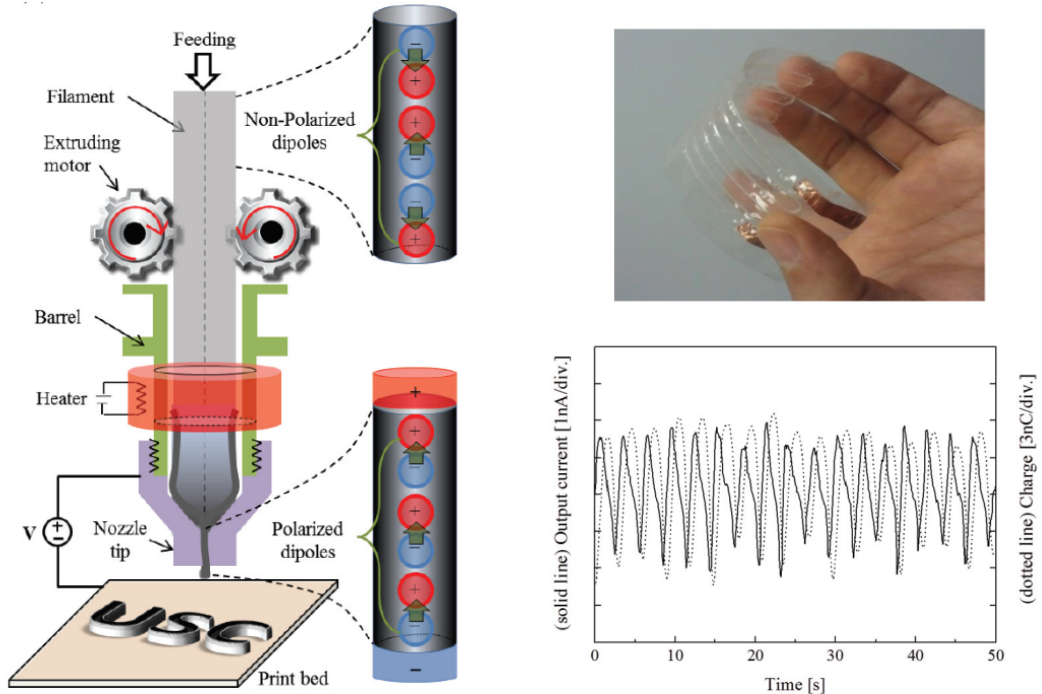


**Figure 14. Illustration of the electric poling-assisted AM method for printing piezoelectric PVDF components (left). Image of printed PVDF device and output current and capacitive charge during flex cycles (right). (Ref 42)**

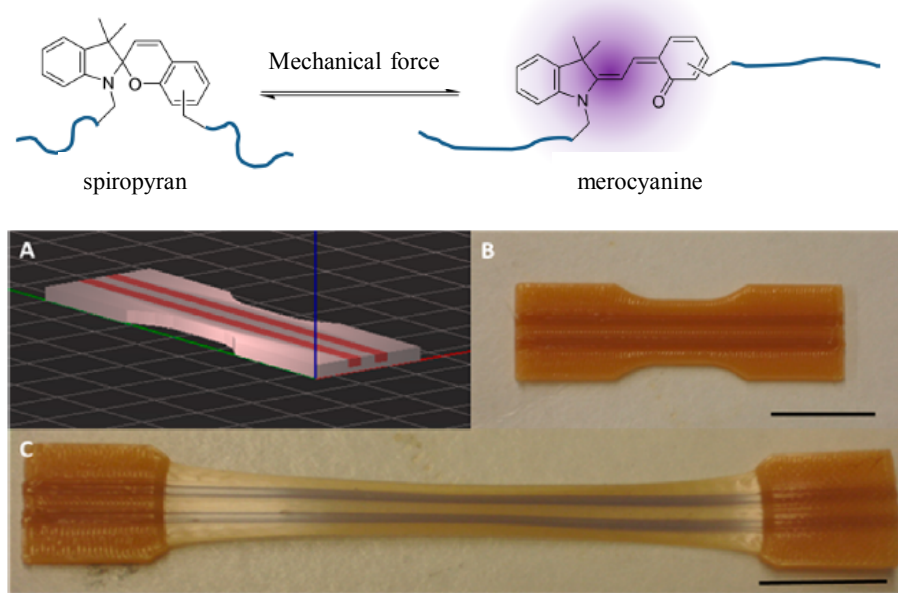


**Figure 15. Schematic of mechanochemical transformation from colorless spiropyran form to the purple colored merocyanine form (top) and images of spiropyran-PCL dog-bones before and after stretching. (Ref 43)**



## 4. MATERIAL PERFORMANCE AND AGING CONSIDERATIONS FOR ADDITIVELY MANUFACTURED POLYMERS

Understanding the aging behavior of organic materials is critical for predicting component lifetime and assessing a component's state-of-health. Irrespective of a particular application, the material processing history, cure state and cure profile, as well as its chemical make-up will affect long-term relaxation and physical properties changes, as well as any chemically driven degradation processes. In particular, chemical degradation is often governed by catalyst residues, trace impurities or otherwise reactive constituents, plus perhaps contributions from any fillers and similar additives. For example, the incorporation of photo-acid generators changing pH conditions, or any left-over photo free radical generators or similar rapid action catalysis will likely change the chemical nature of a material. Similarly, any rapid thermal cure of a two-part reactive resin system will change the underlying polymerization kinetics, resulting cure shrinkage and local conversion state. For all of these reasons, the microscopic chemical and physical attributes of additively manufactured parts are therefore expected to be different from those of bulk materials obtained through traditional processing techniques, i.e. injection molding or mix, cast and cure thermosets. Further, it is also important to recognize that the unique microscopic environment within additive manufactured parts will not only affect initial make-up (i.e. subtle gradients or anisotropy in a material), but also its aging behavior. Understanding the aging behavior of additive manufactured parts will be vital for determining which 3D printing techniques are acceptable for a particular application. Most importantly, we recognize that additive manufacturing or 3D printing beyond simple micro extrusion of specific thermoplastics where perfect strand adhesion is the major issue of concern, involves optimized and likely rapid cure polymer chemistry not commonly used in more traditional material processing and cure strategies. Below we present a preliminary and somewhat speculative discussion of aging considerations for the AM techniques described above.

The chemical properties of FDM (fused deposition modeling) printed parts are identical to the bulk properties since no additional chemical reactions take place during the fabrication process. On the other hand, the microstructure of FDM printed parts can deviate significantly from that of the bulk material. Specifically, FDM parts typically possess a significantly greater surface area due to the limited connectivity of individual filaments. Internal voids due to incomplete filament fusion results in a maximum material penetration depth (distance from the surface of the material to the core) that is close to the radius of an individual cylindrical filament, where typical filaments have radii on the order of 50  $\mu\text{m}$ , and therefore local variations in spatially dependent diffusion pathways. This will lead to significant differences in the oxidative degradation behavior of FDM materials as compared to their bulk material counterparts, since surface and bulk degradation rates often differ due to oxygen permeation rates which depend on the depth of penetration. It is likely that FDM printed parts will exhibit faster and more complete oxidative degradation compared to bulk. Further, built-in porosity diffusion processes can no longer be described by simple Fickian diffusion, but will involve Fickian and Langmuir sorption and diffusion phenomena perhaps all the way to additional pooling of volatile penetrants. Particularly, water sorption and hydrolytic aging may be significantly affected by porosity. Non Fickian and simple Henry's law sorption will also affect the swelling behavior and hence retention of primary physical properties observed for a perfectly homogenous material.

The short cure time that is needed for stereolithography raises concerns about the extent of polymerization and its cure state history (reaction kinetics and initiation versus propagation aspects during molecular weight growth) during layer-by-layer photocuring. In fact, incomplete curing of each layer is often targeted in order to enhance interlayer covalent bonding, which is achieved via a secondary post-print cure process. This may not only lead to initially incomplete curing and complicated cure schedules, leaving reactive groups within the polymer structure which are especially susceptible to ongoing secondary delayed cure reactions, but also enhanced stress built-up over time and adhesive property changes as part of convoluted ‘residual chemistry’ plus physical relaxation phenomena. Understanding how the rapid cure reaction kinetics and resulting polymer network characteristics are related to the printing cure parameters and the post-print cure schedule will be crucial for manufacturing robust and optimized materials.

Reactive direct-write processes are similar to stereolithography in that the effects of reaction kinetics and incomplete curing on long-term material responses must be considered. In addition, the complex materials gradients as part of the processing history that are often relevant to direct-write processes may lead to a more complicated analysis of their aging behavior. For example, Stratasys printers are able to deposit composite resins with pre-determined mechanical properties by adjusting the ratios of monomers in multi-component blends (Stratasys Digital Materials). The network characteristics and extent of curing in these ‘digital materials’ will depend on the reactivity ratios of the two monomers and their molecular interactions in the resin. The aging behavior of such gradient materials is not likely to mimic that of the individual constituents, but rather depend on the unique structure that arises from the blend and its deposition timing. Any anisotropic property as part of the time dependent strand or layer by layer deposition, should a slowly reactive two-part system be used (for example thermally cured silicone), could result in a non-homogenous response with variations in local stress and volume changes subject to water or organic vapor sorption.

In conclusion, we expect the reliability and aging characteristics of 3D printed and additively manufactured materials to be significantly different in comparison with homogeneous and traditionally processed materials. However, there may also be situations where the small scale control over properties in a 3D process may be of long-term benefit and create better performing materials. Advanced 3D and additive manufacturing should ultimately transition to an avenue for printing ‘polymer properties on demand’ with reliability aspects comprehensively addressed as part of material selection, processing history, reaction kinetics, deposition strategies and its final 3D structure. It is clear that this is a broader challenge for advanced materials science, where material chemists, physicists and process engineers will need to join forces to effectively make innovation become reality. As this report has shown, from just the materials chemistry point of view, 3D printing will employ more extreme material solutions, cutting edge cure strategies and optimized reactions kinetics that so far are not easily found in existing materials.

## 5. CONCLUSIONS

Significant advancements in additive manufacturing of polymer materials have been made over the past two decades with printable polymers finding new applications in medicine, electronics, and high performance structural materials. At the same time, a great deal of chemistry remains unexplored for additive manufacturing and the overall material properties that are commercially available are limited. Thermoset polymer chemistry available for additive manufacturing is largely confined to traditional free radical acrylate and cationic epoxide polymerizations, where fast reaction kinetics and tunable viscosities provide a handle for optimizing resin formulations and their deposition features. Still, printing epoxy networks via direct-write has proved challenging due to inadequate slow reaction kinetics. These limitations have motivated interest in developing ‘unconventional’ chemical reactions for AM processes in order to open new opportunities in printable materials. Any reactions that are scalable and are characterized by fast kinetics with few byproducts are potential candidates for AM processing. These requirements suggest that the chemical reactions falling under the category of ‘click chemistry’ are interesting systems to pursue for AM. For example, ‘photo-click’ approaches to efficient reactions such as thiol-ene and alkyne-azide chemistry are intriguing. However, the end-properties of printed polymers must be considered when developing new AM chemistry strategies. Desirable properties that are currently lacking in printable polymer materials include high strength polymers, high elasticity polymers, robust network structures with oxidative stability/long material lifetime, and the capability to incorporate high loading of fillers. In addition, control of the interlayer microstructure is an area that has received little attention, but is vital for ensuring robust structures via layer-by-layer fabrication. For photo-cured systems, interfacial structure may be controlled by formulating hybrid resin systems with two or more components of differing reactivity, such that an initial rapid cure sets the layer and affords initial adhesion, and a secondary cure promotes full structural integrity. Alternatively, supramolecular chemistry may be useful for controlling interfacial interactions. For example, supramolecular resins based on strong complementary hydrogen bonding interactions could promote efficient interlayer interactions.

Lastly, additive manufacturing presents unique materials aging challenges since the microstructure of AM materials differs significantly from their bulk counterparts. Understanding the connection between cure chemistry, AM processing, network structure, and aging mechanisms will enable improved AM materials. It is clear that the field of polymer additive manufacturing is still in the early stages of materials development, and many opportunities exist for expanding the scope of AM polymers. Future developments should be addressed by joint efforts between material chemists, physicists and process engineers to effectively make innovation become reality. As this report has shown, from just the materials chemistry point of view, the trends in 3D printing will employ more niche approaches, and bring new cutting edge cure strategies that so far are not found in existing materials.

## 6. REFERENCES

1. Rowe, C. W.; Pryce Lewis, W. E.; Cima, M. J.; Bornancini, E. R. N.; Sherwood, J. K.; Wang, C.-C.; Gaylo, C. M.; Fairweather, J. A. *PCT Int. Appl.* **2003**: WO 2003041690.
2. Ursan, I.; Chiu, L.; Pierce, A. *J. Am. Pharm. Assoc.* **2013**, *53*, 136-144.
3. (a) Liu, Q.; Leu, M. C.; Schmitt, S. M. *Int. J. Adv. Manuf. Technol.* **2006**, *29*, 317-335. (b) Sun, B. J.; Kennedy, C. R.; Sundar, V.; Lichkus, A. M. *U.S. Pat. Appl. Pub.* **2014**: US 20140131908. (c) Adusumilli, P.; Lech, S. J. *PCT Int. Appl.* **2008**: WO 2008005432.
4. (a) Gauvin, R.; Chen, Y.-C.; Lee, J. W.; Soman, P.; Zorlutuna, P.; Nichol, J. W.; Bae, H.; Chen, S.; Khademhosseini, A. *Biomaterials*, **2012**, *33*, 3824-3834. (b) Rosenzweig, D. H.; Carelli, E.; Steffen T.; Jarzem, P.; Haglund, L. *Int. J. Mol. Sci.* **2015**, *16*, 15118-15135.
5. Horn, T. J.; Harrysson, O. L. A. *Science Progress* **2012**, *95*, 255-282.
6. Gibson, I.; Cheung, L. K.; Chow, S. P.; Cheung, W. L.; Beh, S. L.; Savalani, M.; Lee, S. H. *Rapid Prototyp. J.* **2006**, *12*, 53-58.
7. (a) Liu, B.; Gong, X.; Chappell, W. J. *IEEE Trans. Microw. Theory Techn.* **2004**, *52*, 2567-2575. (b) Espalin, D.; Muse, D. W.; MacDonald, E.; Wicker, R. B. *Int. J. Adv. Manuf. Technol.* **2014**, *72*, 963-978. (c) Lopes, A. J.; MacDonald, E.; Wicker, R. B. *Rapid Prototyp. J.* **2012**, *18*, 129-143.
8. Zhang, C.; Anzalone, N. C.; Faria, R. P.; Pearce, J. M. *PLoS One* **2013**, *8*, e59840.
9. Kitson, P. J.; Rosnes, M. H.; Sans, V.; Dragone, V.; Cronin, L. *Lab Chip* **2012**, *12*, 3267-3271.
10. (a) Shofner, M. L.; Lozano, K.; Rodríguez-Macías, F. J.; Barrera, E. V. *J. Appl. Poly. Sci.* **2003**, *89*, 3081-3090. (b) Ning, F.; Cong, W.; Qiu, J.; Wei, J.; Wang, S. *Composites Part B* **2015**, *80*, 369-378.
11. Leigh, S. J.; Bradley, R. J.; Purssell, C. P.; Billson, D. R.; Hutchins, D. A. *PLoS One* **2012**, *7*, e49365.
12. Satches, M. R. "Nano-Composite material Development for 3-D Printers", SAND2015-8893-T (10/2015)
13. Ray, S.; Easteal, A. J.; Cooney, R. P.; Edmonds, N. R. *Mater. Chem. Phys.* **2009**, *113*, 829-838.
14. Davies, S. J.; Ryan, T. G.; Wilde, C. J.; Beyer, G. *Synth. Met.* **1995**, *69*, 209-210.
15. <http://www.matweb.com/index.aspx>
16. (a) Lee, K.-W.; Wang, S.; Fox, B. C.; Ritman, E. L.; Yaszemski, M. J.; Lu, L. *Biomacromolecules* **2007**, *8*, 1077-1084. (b) Liska, R.; Schuster, M.; Inführ, R.; Turecek, C.; Fritscher, C.; Seidl, B.; Schmidt, V.; Kuna, L.; Haase, A.; Varga, F.; Lichtenegger, H.; Stampfl, J. *J. Coat. Technol. Res.* **2007**, *4*, 505-510. (c) Stampfl, J.; Baudis, S.; Heller, C.; Liska, R.; Neumeister, A.; Kling, R.; Ostendorf, A.; Spitzbart, M. *J. Micromech. Microeng.* **2008**, *18*, 125014. (d) Baudis, S.; Nehl, F.; Ligon, S. C.; Nigisch, A.; Bergmeister, H.; Bernhard, D.; Stampfl, J.; Liska, R. *Biomed. Mater.* **2011**, *6*, 055003.
17. (a) Ge, Q.; Dunn, C. K.; Qi, H. J.; Dunn, M. L. *Smart Mater. Struct.* **2014**, *23*, 094007. (b) Mao, Y.; Yu, K.; Isakov, M. S.; Wu, J.; Dunn, M. L.; Qi, H. J. *Sci. Rep.* **2015**, *5*, 13616.
18. Duoss, E. B.; Weisgraber, T. H.; Hearon, K.; Zhu, C.; Small IV, W.; Metz, T. R.; Vericella, J. J.; Barth, H. D.; Kuntz, J. D.; Maxwell, R. S.; Spadaccini, C. M.; Wilson, T. S. *Adv. Funct. Mater.* **2014**, *24*, 4905-4913.
19. Gratson, G. M.; Lewis, J. A. *Langmuir* **2005**, *21*, 457-464.

20. Tumbleston, J. R.; Shirvanyants, D.; Ermoshkin, N.; Janusziewicz, R.; Johnson, A. R.; Kelly, D.; Chen, K.; Pinschmidt, R.; Rolland, J. P.; Ermoshkin, A.; Samulski, E. T.; DeSimone, J. M. *Science* **2014**

21. <http://3dprint.com/53286/gizmo-3d-printers-fastest/>

22. Kruth, J.-P.; Levy, G.; Klocke, F.; Childs, T. H. C. *Annals of the CIRP* **2007**, *56*, 730-759.

23. Lapin, S. C.; Snyder, J. R.; Sitzmann, E. V.; Barnes, D. K.; Green, G. D. *Stereolithography Using Vinyl Ether-Epoxide Polymers* US Patent US5437964 A **1995**.

24. Yagci, Y.; Jockusch, S.; Turro, N. J. *Macromolecules* **2010**, *43*, 6245-6260.

25. Cokbaglan, L.; Arsu, N.; Yagci, Y.; Jockusch, S.; Turro, N. J. *Macromolecules* **2003**, *36*, 2649-2653.

26. Cumpston, B. H.; Ananthavel, S. P.; Barlow, S.; Dyer, D. L.; Ehrlich, J. E.; Erskine, L. L.; Heikal, A. A.; Kuebler, S. M.; Lee, I.-Y. S.; McCord-Maughon, D.; Qin, J.; Röckel, H.; Rumi, M.; Wu, X. L.; Marder, S. R.; Perry, J. W. *Nature* **1999**, *398*, 51-54.

27. Schafer, K. J.; Hales, J. M.; Balu, M.; belfield, K. D.; Van Stryland, E. W.; Hagan, D. J. *J. Photochem. Photobiol. A* **2004**, *162*, 497-502.

28. (a) Jin, M.; Xu, H.; Hong, H.; Malval, J.-P.; Zhang, Y.; Ren, A.; Wan, D.; Pu, H. *Chem. Commun.* **2013**, *49*, 8480-8482. (b) Zhou, W.; Kuebler, S. M.; Braun, K. L.; Yu, T.; Cammack, J. K.; Ober, C. K.; Perry, J. W.; Marder, S. R. *Science* **2002**, *296*, 1106-1109.

29. Arimitsu, K.; Endo, R. *Chem. Mater.* **2013**, *25*, 4461-4463.

30. Suyama, K.; Shirai, M. *Prog. Polym. Sci.* **2009**, *34*, 194-209.

31. (a) Turner, S. C.; Baudin, G. Photoactivatable nitrogen-containing bases on amino alkenes. Switzerland: PCT Int Appl. Wo: (Ciba Specialty Chemicals Holding Inc.); 1998, pg. 51. (b) Baudin, G.; Dietliker, K.; Jung, T. Photoactivatable nitrogen bases. Switzerland: PCT Int Appl. Wo: (Ciba Specialty Chemicals Holding Inc.); 2003, pg. 62.

32. (a) Salmi, H.; Allonas, X.; Ley, C.; Maréchal, D.; Ak, A. *J. Photopolym. Sci. Tehnol.* **2012**, *25*, 147-151. (b) Suyama, K.; Ogata, S.; Inoue, T.; Shirai, M. *J. Photopolym. Sci. Technol.* **2010**, *23*, 439-446. (c) Ohba, T.; Nakai, D.; Suyama, K.; Shirai, M. *J. Photopolym. Sci. Technol.* **2004**, *17*, 11-14. (d) *Photoinitiated and Thermal Crosslinking of Epoxides using Oxime-Blocked 2-Isocyanato-Ethyl-Methacrylate* **2003**, 7<sup>th</sup> Nurnberg Congress, European Coatings Show, Nurnberg, Germany.

33. Sangermano, M.; Vitale, A.; Dietliker, K. *Polymer* **2014**, *55*, 1628-1635.

34. Arimitsu, K.; Fuse, S.; Kudo, K.; Furutani, M. *Mater Lett.* **2015**, *161*, 408-410.

35. Moses, J. E.; Moorhouse, A. D.; *Chem. Soc. Rev.* **2007**, *36*, 1249-1262.

36. Hayase, K.; Zepp, R. G. *Environ. Sci. Technol.* **1991**, *25*, 1273.

37. Dadashi-Silab, S.; Yagci, Y. *Tetrahedron Lett.* **2015**, *56*, 6440-6443.

38. Adzima, B. J.; Tao, Y.; Kloxin, C. J.; DeForest, C. A.; Anseth, K. S.; Bowman, C. N. *Nat. Chem.* **2011**, *3*, 256-259.

39. Shih, H.; Lin, C.-C. *Biomacromolecules* **2012**, *13*, 2003-2012.

40. Leonards, H.; Engelhardt, S.; Hoffmann, A.; Pongratz, L.; Schriever, S.; Blasius, J.; Wehner, M.; Gillner, A. *Advantages and Drawbacks of Thiol-Ene Resins for 3D-Printing*. 2<sup>nd</sup> Meeting of the Laser 3D Manufacturing: **2015**, 9353, UNSP 93530F.

41. (a) Wang, Y.; Song, W.; Hu, W. J.; Lin, Q. *Angew. Chem. Int. Ed.* **2009**, *48*, 5330-5333. (b) Yu, Z.; Lin, Q. *J. Am. Chem. Soc.* **2014**, *136*, 4153-4156.

42. Cooperstein, I.; Layani, M.; Magdassi, S. *J. Mater. Chem. C* **2015**, *3*, 2040-2044.

43. Lee, C.; Tarbutton, J. A. *procedia Manufacturing* **2015**, *1*, 320-326.

44. Peterson, G. I.; Larsen, M. B.; Ganter, M. A.; Storti, D. W.; Boydston, A. J. *ACS Appl. Mater. Interfaces* **2015**, 7, 577-583.

## Distribution

1	MS-0346	Ford, Kurtis R.	1526
1	MS-0481	Neidigk Matthew A.	2224
1	MS-0840	Long, Kevin N.	1554
1	MS-0885	Valley, Michael	1810
1	MS-0885	Wall, Frederick D.	1850
1	MS-0885	Smith, Mark F.	1801
1	MS-0887	Aselage, Terrence L.	1800
1	MS-0888	McElhanon, James R.	1853
1	MS-0888	Bernstein, Robert	1853
1	MS-0888	Jones, Brad H.	1853
1	MS-0888	Stinnett, Regan W.	1854
1	MS-0888	Serna, Lysle M.	1852
1	MS-0889	Hochrein, James M.	1831
1	MS-0889	Helean, Katheryn B.	1852
1	MS-0958	Kelly, Michael J.	1833
1	MS-0958	Hibbs, Michael	1833
1	MS-0958	Kropka, Jamie M.	1853
1	MS-0958	Wyatt, Nicholas B.	1853
1	MS-1349	Cook, Adam W.	1832
1	MS-1411	Black, Hayden T.	1853
1	MS-1411	Celina Mathias C.	1853
1	MS-1411	Giron, Nicholas H.	1853
1	MS-1411	Redline, Erica M.	1853
1	MS-1454	Minier, Leanna M. G.	2554
1	MS-1455	Brotherton, Christopher M.	2555
1	MS-1455	Rodacy, Philip J	2555
1	MS-0899	Technical Library	9536





**Sandia National Laboratories**